scientific reports

Check for updates

OPEN

The circDUSP1/miR-429/DLC1 regulatory network affects proliferation, migration, and invasion of triple-negative breast cancer cells

Canhui Jian[1,2], Xiaoxue Tian[1,2], Shuai Luo[1], Jiafei Zeng[1], Jin Li[1], Ting Xu[2] & Jinjing Wang[1,2]✉

Triple-negative breast cancer (TNBC) is an aggressive subtype lacking effective targeted therapies, with circular RNAs (circRNAs) emerging as key regulators in cancer progression through competitive endogenous RNA (ceRNA) networks. Although circRNAs function as miRNA sponges in TNBC, the specific role of circDUSP1 in the miR-429/DLC1 pathway remains unknown. In this study, a circular RNA, circDUSP1, was identified as differentially expressed in TNBC using an online database. Using TNBC patient tissues and cell lines (MDA-MB-231/MDA-MB-468), we quantified circDUSP1 expression via qRT-PCR. The molecular characteristics of circDUSP1 were identified through methods such as nuclear-cytoplasmic separation, RNase R digestion, and FISH. Assessed the impact of circDUSP1 on TNBC cell proliferation/migration/invasion through functional assays (CCK-8, colony formation, Transwell, etc.). The circDUSP1/miR-429/DLC1 regulatory network's role in TNBC was validated using dual-luciferase reporter gene, RNA pull-down, and rescue assays. circDUSP1 was significantly downregulated in TNBC tissues and cell lines. circDUSP1 overexpression suppressed TNBC cell proliferation, migration, invasion, and tumor growth in vivo circDUSP1 directly bound miR-429 to relieve its repression of tumor suppressor DLC1 miR-429 mimics attenuated circDUSP1-mediated tumor suppression. circDUSP1 inhibits TNBC progression by acting as a molecular sponge for miR-429 to upregulate DLC1. This regulatory network represents a novel therapeutic target for TNBC.

Keywords TNBC, Triple-negative breast cancer, circDUSP1, miR-429, DLC1

Breast cancer ranks among the most prevalent malignancies affecting women globally, with its incidence steadily rising, posing a significant threat to women's health. Triple-negative breast cancer (TNBC) is a distinct and heterogeneous subtype lacking the three primary targets: estrogen receptor (ER), progesterone receptor (PR), and human epidermal growth factor receptor 2 (HER-2)[1]. Consequently, patients do not benefit from existing endocrine and targeted therapies. Chemotherapy remains the primary treatment for TNBC[2], yet its effectiveness is limited, and prognosis remains poor. Recently, the combination of cytotoxic drugs with immune checkpoint inhibitors and antibody-drug conjugates has emerged as a promising treatment avenue[2]. However, no targeted drugs for TNBC have received approval from the U.S. Food and Drug Administration (FDA). Thus, investigating the molecular mechanisms of TNBC and identifying new biomarkers and targets are crucial for enhancing patient survival and prognosis, offering innovative treatment strategies.

circular RNA (circRNA), a novel class of non-coding RNA, plays a crucial regulatory role in cancer development. Formed from pre-mRNA via back splicing, circRNAs possess a closed-loop structure and are abundant in microRNA (miRNA) binding sites[3]. Dysregulation of circRNA can promote tumorigenesis and metastasis, making it a promising target for cancer therapy[4]. Numerous studies have linked circRNA to tumor cell proliferation, apoptosis, and metastasis[5]. Notably, circRNAs exhibit high stability and specificity and can modulate miRNA activity through the competing endogenous RNA (ceRNA) mechanism[4], influencing downstream gene expression[6]. circDUSP1 (circBase ID: hsa_circ_0075043), originating from exon 4 of the dual-specificity phosphatase 1 (DUSP1) gene, is a circular transcript of 1043 nucleotides formed by back

[1]Department of Pathology, Affiliated Hospital of Zunyi Medical University, Zunyi 563003, Guizhou Province, China. [2]Department of Pathology, School of Preclinical Medicine, Zunyi Medical University, Zunyi 563000, Guizhou Province, China. ✉email: jinjingwangls@163.com

splicing. Research indicates that circDUSP1 expression is reduced in TNBC and inversely correlates with TNBC tumorigenesis and progression[7].

miRNAs are a class of conserved endogenous non-coding single-stranded RNAs, approximately 1825 nucleotides in length, prevalent in eukaryotes and highly conserved across species. miRNAs regulate post-transcriptional gene expression by binding to the 3' untranslated region (3'UTR) of target mRNAs through base pairing. They function as oncogenes or tumor suppressors[8], influencing tumor cell survival, proliferation, invasion, metastasis, apoptosis, and drug response[9]. Consequently, miRNAs hold significant potential for early tumor diagnosis, prognosis, and therapeutic target development. Our previous research indicates that miR-429 is markedly overexpressed in TNBC, enhancing TNBC cell proliferation, migration, and invasion by targeting DLC1 (Deleted in Liver Cancer 1)[10,11].

DLC1 is a crucial tumor suppressor gene[12] within the Rho GTPase-activating protein (RhoGAP) family, known for inhibiting Rho GTPase activity[13]. As a GTPase-activating protein, DLC1 is pivotal in processes like cell migration and proliferation by terminating RhoGTPase signaling and regulating cytoskeletal reorganization and RhoGTPase pathways[14]. Beyond its role as a tumor biomarker, DLC1 is a promising therapeutic target with significant clinical implications. Our previous research demonstrated that DLC1 is underexpressed in TNBC and is regulated by miR-429. Based on the principle of the ceRNA mechanism, circDUSP1 could potentially upregulate DLC1 expression by sponging miR-429. Currently, the specific interactions among circDUSP1, miR-429, and DLC1 remain unexplored. This study aims to elucidate the mechanisms involving circDUSP1, miR-429, and DLC1 in TNBC using molecular techniques, offering new molecular targets for TNBC prediction and treatment. Currently, the specific molecular interactions and regulatory relationships among circDUSP1, miR-429, and DLC1 remain unexplored.

Therefore, this study aims to: Determine the clinical relevance and functional role of circDUSP1 in TNBC progression. Elucidate the molecular mechanism of the circDUSP1/miR-429/DLC1 regulatory network. Evaluate the therapeutic potential of targeting this axis for TNBC treatment.

Methods

Tissue samples

Freshly resected tissue specimens were obtained from three patients diagnosed with TNBC, with pathologic confirmation, at the Affiliated Hospital of Zunyi Medical University. The samples included three pairs of cancerous and adjacent normal breast tissues. All patients were newly diagnosed with breast cancer and had not undergone prior radiotherapy or chemotherapy. Informed consent was obtained from each participant before surgery, and the study received approval from the hospital's Research Ethics Committee. Post-surgical samples were immediately stored in liquid nitrogen.

Cell culture

Human mammary epithelial cells (MCF-10A), TNBC cells (MDA-MB-231 and MDA-MB-468), and HEK-293T cells were sourced from Procell. MCF-10A cells were cultured in a specialized MCF-10A medium (Procell, China), while MDA-MB-231 and MDA-MB-468 cells were maintained in high-glucose DMEM (Procell, China) supplemented with 10% FBS and 1% penicillin-streptomycin. Cell lines were cultured in an incubator with 5% CO_2 at 37 °C.

All cell lines were authenticated by commercial short tandem repeat (STR) profiling (Genetica Cell Line Testing) and confirmed ≥ 95% match to reference databases (ATCC/DSMZ). Cells were routinely tested for mycoplasma contamination via PCR-based detection (Venor®GeM Mycoplasma Detection Kit, Minerva Biolabs) every 3 months, and all experiments conducted within 2 months of the latest negative test.

Cell transfection

Lentiviral transfection was performed using knockdown lentiviruses (Lv-NC-sh, Lv-hsa-circDUSP1-sh) and overexpression lentiviruses (Lv-NC-oe, Lv-hsa-circDUSP1-oe), synthesized by Fenghui Biotechnology Co., Ltd. Virus titers and MOI values are found in Supplementary File S4.Twenty-four hours before transfection, adherent cells were plated in 6-well plates at 1×10^5 cells per well and incubated overnight under standard conditions (37 °C, 5% CO_2). After reaching 50% confluence, the medium was replaced with 2 mL fresh medium (0.5 μg/mL polybrene), and lentiviral solution was added. The cells were then incubated under the same conditions for 48 h. Afterward, the viral-containing medium was replaced with fresh culture medium, and successful transfection was confirmed by the appearance of green fluorescence in over 80% of the cells under a fluorescence microscope. At this point, the medium was replaced with culture medium supplemented with 2 μg/mL puromycin, with daily observation and medium replacement. Once all cells in the blank control group had died, the infected cells were expanded to establish a stable transfected cell line.

The RNA of hsa-miR-429 mimics, hsa-miR-429 inhibitors, and their respective negative controls (NC) were synthesized by Sangon Biotech Co., Ltd. (Shanghai). TNBC cell lines with stably expressing knockdown or overexpression of circDUSP1 were seeded into 6-well plates and incubated for 24 h. Subsequently, two 1.5 mL sterile EP tubes were prepared: 100 μL of serum-free medium was added to each, with 100 nm RNA placed in one tube and 12 μL of enhanced transfection reagent (Biodragon, China) in the other. After 5 min of incubation, the contents of both tubes were combined and allowed to stand for 20 min. The resulting mixture was then added to the appropriate wells of the 6-well plate and incubation was continued for 48 h. The transfected cells were collected, transfection efficiency was verified, and successful transfection was confirmed before conducting experiments.

Quantitative real-time PCR (qRT-PCR)

Total RNA was extracted using the Beyotime kit (China), then reverse-transcribed into cDNA with Takara's PrimeScript Reverse Transcription Kit (Takara Bio, China). cDNA amplification was carried out using either the TB Green PCR Kit or the TB Green Master Mix Kit (both from Takara Bio, China). GAPDH was used as the internal reference gene for circDUSP1 and DLC1 mRNA expression, and U6 was used as the internal reference gene for miR-29 expression. . The 2^(-ΔΔCt) method was employed to obtain relative expression. Primer sequences are provided in Table 1.

RNase R digestion

Total RNA was extracted using the RNA extraction kit and divided into two equal aliquots (1 μg/aliquot). One aliquot was left untreated, while RNase R (Epicentre, USA) was added to the other, with incubation at 37 °C for 20 min for digestion. Both undigested and digested RNA samples were analyzed viaqRT-PCR to quantify the expression levels of circDUSP1 and DUSP1. Genes from the control group were used as internal references, and relative gene expression was assessed by the 2^(-ΔCt) method.

Nucleocytoplasmic separation assay

Cell pellets were harvested, and nuclear and cytoplasmic fractions were isolated using a nuclear protein extraction kit (Solarbio, China). Total RNA was subsequently extracted, and the expression of circDUSP1 in both the nucleus and cytoplasm was quantified via qRT-PCR. KRT19P3 and GAPDH were employed as internal controls for the nucleus and cytoplasm, respectively. The target gene's relative expression was obtained in each compartment (2^(-ΔCt) method).

Extraction of cell genomic DNA (gDNA)

To confirm that the detected circRNA signal was not from gDNA contamination or linear RNA splice variants, we extracted gDNA from TNBC cells using an animal tissue/cell gDNA extraction kit (Solarbio, China). The expression levels of circDUSP1, DUSP1, and GAPDH were analyzed via qRT-PCR. Divergent primers for circDUSP1 were designed and synthesized by Sangon Biotech Co., Ltd. (Shanghai), with primer sequences provided in Table 1.

Agarose gel electrophoresis

The cDNA and gDNA amplification products from the preceding experiment were analyzed via agarose gel electrophoresis. A 40 mL solution of 3% agarose gel was prepared and allowed to cool naturally to approximately 60 °C. Nucleic acid dye was then added at a ratio of 1:5000 (v/v), mixed thoroughly, and the solution poured into a gel casting tray with a comb, where it was left to solidify at room temperature. After the gel solidified, the comb was removed, and the gel was transferred to an electrophoresis chamber filled with 1× TBE buffer. The 6× loading buffer was diluted to 1×, and the PCR products were further diluted 1:1 with the 1× loading buffer. Both the marker and the diluted samples were loaded into the gel wells. Electrophoresis was initiated immediately after loading. Upon completion, the gel was visualized and photographed using a UV gel imaging system.

Fish

circDUSP1 and miR-429 FISH probes were designed and synthesized by GenePharma Pharmaceutical Co., Ltd. (Shanghai), with the probe sequences detailed in Table 2. Localization of circDUSP1 in TNBC cells was assessed using the RNA FISH kit (GenePharma). Briefly, fixed and permeabilized cell slides were pre-hybridized in hybridization buffer at 55 °C for 2 h. The probes in hybridization buffer were denatured at 75°C for 5 min (PCR instrument). Denatured probe mixture was applied to the cell slides and hybridized at 42°C for 24 h in a

Gene	Primer sequence (5′-3′)
circDUSP1	F: 5'-CACCATCTGCCTTGCTTACCTTATG- 3' R: 5'-GCTTCGCCTCTGCTTCACAAAC- 3'
circDUSP1 Divergent primers	5'-CTGGACGAGGCCTTTGAGTT- 3'
miR-429	F: 5'-CGCGCGTAATACTGTCTGGTAA- 3' R: 5'-AGTGCAGGGTCCGAGGTATT- 3'
miR-429 stem-loop primers	5'-GTCGTATCCAGTGCAGGGTCCGAGGTATTCGCACTGGATACGACACGGTT- 3'
DLC1	F: 5'-CGAGATCTTCCTGAGCCACTAAT- 3' R: 5'-GCTGTGACATCGCTCAGGAAATA- 3'
DUSP1	F: 5'-ACCACCACCGTGTTCAACTTC- 3' R: 5'-TGGGAGAGGTCGTAATGGGG- 3'
GAPDH	F: 5'-GAAGGTGAAGGTCGGAGTC- 3' R: 5'-GAAGATGGTGATGGGATTTC- 3'
U6	F: 5'-CCAGTTGTAGGTCGTTCTCAAG- 3' R: 5'-CCAGTTGTAGGTCGTTCTCAAG- 3'
U6 stem-loop primers	5'-GTCGTATCCAGTGCAGGGTCCGAGGTATTCGCACTGGATACGACAAAATATGG- 3'
KRT19P3	F: 5'-CAGTGAGAGGCAGAATCAGG- 3' R: 5'-TTGGAGGTGGACAGGCTATT- 3'

Table 1. Primer sequences for qRT-PCR.

Gene	Primer sequence (5′-3′)
circDUSP1 FISH probe	5'-CCAGCATTCTTGATGGAGTTTGAAA- 3'
miR-429 FISH probe	5'-CCAGCATTCTTGATGGAGTTTGAAA- 3'
circDUSP1 Biotin probe	CCAGCATTCTTGATGGAGTTTGAAA

Table 2. FISH and biotin probe synthesis sequence.

dark humid chamber. Slides were washed twice with 1× SSC/0.1% Tween-20 (5min/wash). Following this, cell nuclei were stained with DAPI (5 min) and observed under a fluorescence microscope.

CCK-8 assay

Stable transfected TNBC cell lines (2×10^3 cells/well) were seeded in 96-well plates. After 24 h of serum starvation, cell proliferation was assessed at 0, 24, 48, 72, and 96 h using CCK-8 reagent (GLPBIO, China). At each time point, culture medium was replaced with fresh medium containing 10% (v/v) CCK-8 solution. Following a 90-minute incubation at 37 °C in the dark, absorbance at 450 nm was measured with an ELISA reader.

Colony formation assay

Stably transfected TNBC cells lines were seeded into 6-well plates at a density of 600 cells per well, followed by the addition of 2 mL complete culture medium with thorough mixing. The plates were then incubated in a humidified cell culture incubator. The culture medium was replaced with fresh complete medium every 3 days. Visible colonies emerged 13 days post-seeding. The colonies were gently washed with PBS and fixed with 4% paraformaldehyde for 15 min. After fixation, the colonies were stained with crystal violet solution for 10 min, followed by PBS washes to remove residual dye. Microscopic images were captured for documentation, and the number of colonies was quantitatively analyzed using Image J software.

EdU proliferation assay

Stably transfected TNBC cells were seeded into 24-well plates at 1×10^5 cells/well. After 24 h of standard culture, prewarmed EdU working solution (BeyoClick™ EdU-594 Cell Proliferation Detection Kit, Beyotime, China) was added, and cells were incubated for 12 h. Following EdU labeling, cells were fixed, permeabilized, and treated with an appropriate volume of Click reaction solution. Cells were incubated in the dark for 30 min, after which the nuclei were counterstained with DAPI. Fluorescence microscopy was used for observation.

Wound healing assay

Before the experiment, draw two parallel reference lines on the bottom of a 6-well plate using a Marker pen. Stably transfected TNBC cells were seeded into 6-well plates at 4×10^5 cells/well for 24 h. At this point, the cells should cover the well bottom. Using a sterile 10 μL sterile pipette tip to create a scratch perpendicular to the reference line, with the intersection points serving as fixed detection points. PBS washing was performed, supplied with serum-free medium, and capture an image of the scratch (record this as the 0-hour scratch area). After incubating in the incubator for another 24 h, wash twice with PBS and capture the image from fixed detection points under a microscope. Four fields of view were captured per well. Use Image J software to measure the scratch area at each time point and calculate the healing rate.

Transwell assay

Stably transfected TNBC cells were digested, centrifuged, and resuspended in serum-free DMEM. Add 200ul of cell suspension with a cell density of 1×10^5/mL to the upper chamber of an 8 μM Transwell, with DMEM containing 12% FBS in the lower chamber. After 24 h of incubation, the upper chamber was removed, and non-migrated cells were gently wiped off with a cotton swab. Migrated cells on the membrane underside were fixed with 4% paraformaldehyde, stained with 0.1% crystal violet for 5 minutes, imaged under a microscope, and quantified using ImageJ software.

For the invasion assay, a 0.5 mg/mL matrix gel (pore size 8 μM, Corning, USA) was pre-coated on the upper chamber of the Transwell. Other steps followed the same procedure as in the migration assay after the gel had solidified.

Dual-luciferase reporter gene assay

The psi-CHECK2-circDUSP1-WT and psi-CHECK2-circDUSP1-Mut vectors were synthesized by Sangon Biotech Co., Ltd. (Shanghai). Approximately 6×10^4 293T cells were plated in a 24-well plate and cultured for 24 h. Subsequently, 50 μL of DMEM was mixed with 0.4 μg of WT or MUT plasmid and 1 μL of 20 pmol/μL hsa-miR-429 mimics or miR-429 mimics-NC, incubating for 30 min (solution A). Separately, 48 μL of DMEM was combined with 2 μL of transfection reagent (solution B). Mix both solutions, incubate for 30 min, and add to cells. After 48 h of incubation, luciferase activity was measured using the Dual-Luciferase Reporter Gene Detection Kit (Sangon Biotech, Shanghai, E608001).

RNA-pull down assay

Biotin-labeled circDUSP1 and control probes were synthesized by GenePharma Pharmaceutical Co., Ltd. (Shanghai). Following cell lysis with lysis buffer, the RNA-protein binding reaction mixture was prepared, and the RNA complex was incubated with the biotin-labeled circDUSP1 probe at room temperature for 1 h. The

biotin-labeled RNA complex was then incubated with Streptavidin Magnetic Beads (BEAVER, Suzhou, China) for an additional hour. The magnetic beads bound to the biotin-labeled RNA complex were isolated using a magnetic stand, followed by elution with elution buffer. The RNA complex was collected, and total RNA was extracted for subsequent detection of circDUSP1 and miR-429 enrichment via qRT-PCR.

Western blot

Total protein from TNBC cells was extracted by RIPA lysis buffer (EpiZyme, PC101, Shanghai, China). Protein concentration was tested with the BCA kit (EpiZyme, PC101, Shanghai, China). Proteins were resolved by 7.5% SDS-PAGE (EpiZyme, PG114, Shanghai, China) and transferred to PVDF membranes (0.45 μM, Merck, GER). The membranes were blocked for 30 min at room temperature using a rapid blocking solution. Overnight incubation with rabbit primary antibodies targeting DLC1 and β-actin was performed at 4 °C, followed by incubation with secondary HRP-linked antibodies (1:50000, HUABIO, China) by DLC1 antibody (1: 1000, Abcam, USA) and β-actin (HUABIO, 1: 40000, China) for 1 h. Afterward, the membrane was developed using ECL solution and imaged with a gel imager. Data analysis was conducted with ImageJ.

In vivo tumor growth assay

Three-week-old female BALB/C nude mice were purchased from Chongqing Tengxin Huafu Laboratory Animal Sales Co., Ltd. MDA-MB-231 cells with stable overexpression or knockdown of circDUSP1 were injected subcutaneously into the axillary region of each mouse (5 mice per group), with 100 μL of cell suspension (containing 3×10^6 cells) administered per mouse. Tumor volume was measured weekly. After 30 days, all mice were euthanized via tail vein injection of 3% pentobarbital sodium solution. Upon confirmation of unconsciousness and absence of pain response, complete euthanasia was ensured by cervical dislocation. And the tumors were excised for measurement of tumor weight. The tumor volume was calculated using the formula: Volume (mm^3) = 0.5 × Length × $Width^2$.

HE and Immunohistochemical staining (IHC)

HE staining: Paraffin-embedded sections were dewaxed, rehydrated, and stained with hematoxylin to visualize nuclei and eosin for cytoplasmic staining. Sections were then dehydrated and mounted.

IHC staining involved rehydrating dewaxed paraffin sections and performing antigen retrieval with sodium citrate buffer. Endogenous peroxidase activity was inhibited by a 15-minute incubation with 3% hydrogen peroxide. Then, block sections by 10% goat serum for 30 min. Primary and secondary antibodies were applied in sequence. DBA chromogen was added for 2 min, followed by a 3-minute rinse under running water. The sections were counterstained by hematoxylin, dehydrated, and mounted using graded ethanol. DLC1 cytoplasmic staining (1:100, Abcam, USA) was considered positive. The average optical density of DLC1 was quantified using ImageJ 6.4 software.

Statistic analysis

Statistical analysis utilized GraphPad Prism 9.5, presenting data as mean ± standard deviation ($\overline{x} \pm s$). Group comparisons employed t-tests or one-way ANOVA, with statistical significance set at $p < 0.05$. Significance levels were indicated as follows: * for $p < 0.05$, ** for $p < 0.01$, *** for $p < 0.001$, **** for $p < 0.0001$, and ns for $p \geq 0.05$.

Results

circDUSP1 level was decreased in TNBC tissues and cells

Initial studies revealed elevated expression of miR-429 in TNBC tissues and cells, with evidence supporting a targeted regulatory relationship between miR-429 and DLC1 that influenced TNBC cell processes[10,11]. To investigate the upstream regulatory mechanism of miR-429 in TNBC through DLC1 targeting, online databases such as *circRNADisease.V2.0* (http://cgga.org.cn:9091/circRNADisease/), *StarBase* (https://rnasysu.com/encori/index.php), and *circBank* (http://www.circbank.cn) were utilized to identify circRNAs that were underexpressed in breast cancer and could potentially interact with miR-429. A Venn diagram intersection analysis revealed four candidate circRNAs: circCDYL, circDUSP1, circPTK2, and circSMAD2 (Fig. 1A). Notably, circDUSP1 had been documented to be significantly downregulated in TNBC and linked to patient prognosis[7]. *StarBase* predictions confirmed a binding site between circDUSP1 and miR-429 (Fig. 1B), leading to the selection of circDUSP1 as the focal point for subsequent investigations.

This study analyzed tissue samples from three pairs of TNBC patients using qRT-PCR. The results demonstrated lower levels of circDUSP1 in tumor tissues (Fig. 1C). Furthermore, circDUSP1 expression was downregulated in TNBC cell lines (MDA-MB-231 and MDA-MB-468) (Fig. 1D), consistent with previous reports. According to the circBase database, the full-length sequence of circDUSP1 spans 1043 bp and is derived from the 5' and 3' ends of exon 4 of the DUSP1 gene on chromosome 5 through reverse splicing. Specific primers targeting the reverse splicing junction of circDUSP1 were designed, and the qRT-PCR products underwent Sanger sequencing, confirming the reverse splicing formation of circDUSP1 (Fig. 1E). cDNA and gDNA were extracted from MDA-MB-231 and MDA-MB-468 cells, respectively, and amplified by qRT-PCR, followed by agarose gel electrophoresis. The results revealed that circDUSP1 was only detected in the cDNA samples (Fig. 1F), confirming that the reverse-spliced product of circDUSP1 originated from pre-RNA and was absent from the gDNA. RNase R digestion experiments further confirmed that circDUSP1 exhibited higher resistance to RNase R and greater stability than linear DUSP1 mRNA (Fig. 1G). Nuclear-cytoplasmic separation and FISH assays revealed that circDUSP1 was primarily localized in the cytoplasm (Fig. 1H, I). Results demonstrate that circDUSP1 is downregulated and exhibits exceptional stability in TNBC.

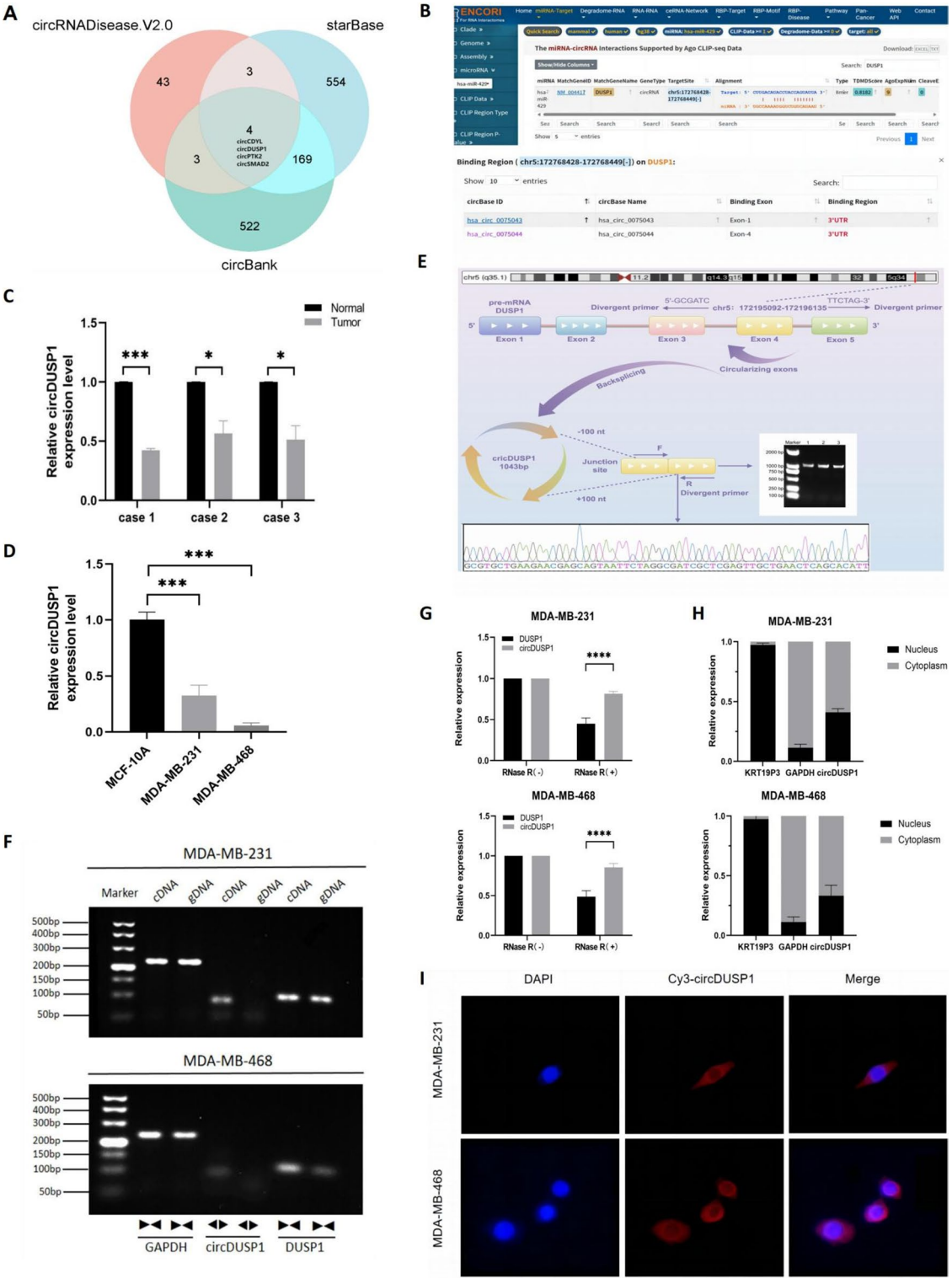

Fig. 1. circDUSP1 level was decreased in TNBC tissues and cells. (A) Venn diagram of circRNAs that are low expressed in breast cancer and can bind to miR-429 in online databas. (B) *starBase* database prediction that the binding of circDUSP1 to miR-429. (C) qRT-PCR analysis showing the relative expression of circDUSP1 in TNBC tissues and normal adjacent tissues. (D) qRT-PCR assessment of circDUSP1 expression levels in the human normal breast epithelial cell line (MCF-10A) and TNBC cell lines (MDA-MB-231, MDA-MB-468). (E) Diagram of circDUSP1 structure and sequencing results. (F) qRT-PCR product agarose gel electrophoresis of circDUSP1. (G) The relative expression levels of circDUSP1 and DUSP1 after RNase R digestion were evaluated by qRT-PCR. (H) qRT-PCR analysis was employed to assess the relative expression levels of circDUSP1, GAPDH, and KRT19P3 in the nucleus and cytoplasm of MDA-MB-231 and MDA-MB-468 cells. (I) The FISH assay was employed to assess the subcellular localization of circDUSP1 in TNBC cells (600×; Scale bar: 20 μM).

circDUSP1 suppressed proliferation and metastasis of TNBC cells in vitro

To assess the impact of circDUSP1 on the biological behavior of TNBC cells, in vitro functional assays were conducted. MDA-MB-231 and MDA-MB-468 cells were stably transfected with circDUSP1 overexpression lentivirus (circDUSP1) and circDUSP1 knockdown lentivirus (si-circDUSP1), respectively. The efficiency of circDUSP1 overexpression and knockdown was confirmed by qRT-PCR (Fig. 2A). CCK8, colony formation, and EdU were employed to evaluate the effect of circDUSP1 on cell proliferation. Results showed that circDUSP1 knockdown promoted cell proliferation, while its overexpression suppressed proliferation (Fig. 2B-F). Furthermore, Transwell and wound healing assays revealed that circDUSP1 overexpression reduced cell migration and invasion, whereas circDUSP1 knockdown exerted the opposite effect (Fig. 2G-L). These data indicate that circDUSP1 inhibits the proliferation, migration, and invasion of TNBC cells in vitro.

circDUSP1 suppressed tumor growth in TNBC in vivo

To assess the impact of circDUSP1 on tumor growth in vivo, MDA-MB-231 cells stably overexpressing or knocking down circDUSP1 were subcutaneously injected into female nude mice. Tumor volume and weight were significantly reduced in the circDUSP1 overexpression group, while they were markedly increased in the circDUSP1 knockdown group (Fig. 3A -C). Immunohistochemical analysis of the Ki-67 proliferation index revealed low Ki-67 expression in tumors from the circDUSP1 overexpression group, whereas tumors from the circDUSP1 knockdown group exhibited significantly higher Ki-67 positivity (Fig. 3D, E). Examination of DLC1 expression via immunohistochemistry showed a notable increase in DLC1 levels in tumors from the circDUSP1 overexpression group, while DLC1 expression was significantly reduced in the knockdown group (Fig. 3D and F). Additionally, qRT-PCR analysis of circDUSP1, miR-429, and DLC1 expression in the tumor tissues confirmed that in the overexpression group, circDUSP1 expression was elevated, miR-429 was downregulated, and DLC1 mRNA levels were upregulated, whereas the knockdown group showed the opposite trend (Fig. 3G-I). These results support the conclusion that circDUSP1 suppresses tumor growth in vivo. In summary, both in vitro and in vivo data confirm the tumor suppressor role of circDUSP1 in TNBC cells.

In TNBC, circDUSP1 functioned as a molecular sponge by binding miR-429

The binding site of circDUSP1 and miR-429 was first predicted using the online tool *Circular RNA Interactome*, and a schematic diagram of this interaction was constructed (Fig. 4A). Subcellular localization of circDUSP1 and miR-429 in TNBC cells was then confirmed through FISH experiments. The circDUSP1 probe was labeled with Cy3 (red fluorescence), while the miR-429 probe was labeled with FAM (green fluorescence). Results showed that in MDA-MB-231 and MDA-MB-468 cells, circDUSP1 and miR-429 co-localized in the cytoplasm (Fig. 4B), supporting the potential for a ceRNA mechanism.

For the Dual-luciferase reporter assay designed to assess the direct binding between circDUSP1 and miR-429, the experimental construct involved cloning the predicted miR-429 binding site(s) from the circDUSP1 sequence into the luciferase reporter plasmids (psi-CHECK2). The binding effect was assessed by measuring luciferase activity. The results show that when circDUSP1 has a mutation at the miR-429 site, there is no significant change in luciferase activity after adding miR-429 mimics compared to the miR-429 mimics-NC group. However, when circDUSP1 does not have a mutation at the miR-429 site, the relative luciferase activity decreases after adding miR-429 mimics compared to the miR-429 mimics-NC group. These findings indicate that circDUSP1 can directly bind to miR-429 (Fig. 4C).

To further validate this interaction, RNA pull-down assays using biotinylated circDUSP1-specific probe were performed. The results demonstrated that circDUSP1 probes significantly enriched circDUSP1 and miR-429 compared to a negative control probe in both cells (Fig. 4D, E). Additionally, qRT-PCR results showed that stable overexpression of circDUSP1 decreased miR-429 expression, while circDUSP1 knockdown increased miR-429 expression (Fig. 4F). Collectively, these data confirm that circDUSP1 regulates miR-429 through the ceRNA mechanism.

circDUSP1 regulated proliferation, migration, and invasion of TNBC cells via the miR-429/DLC1 regulatory network

Prior work established that miR-429 was overexpressed in TNBC tissues and cells (MDA-MB-468), promoting these cell processes, while inhibiting the tumor-suppressive function of DLC1[10,11]. Preliminary data also indicated an interaction between circDUSP1 and miR-429. To investigate the regulatory relationship among circDUSP1, miR-429, and DLC1, the impact of circDUSP1 on DLC1 expression was assessed via qRT-PCR and Western blot. Overexpression of circDUSP1 caused a significant increase in mRNA and protein levels of DLC1, while silencing circDUSP1 resulted in a marked reduction in DLC1 expression at both the mRNA and protein levels (Fig. 5A-C). In vivo experiments also corroborated these observations, revealing corresponding increases or decreases in DLC1 mRNA levels in tumor tissues with stable overexpression or knockdown of circDUSP1 (Fig. 3F). These consistent results from both in vitro and in vivo experiments further supported that circDUSP1 regulated DLC1 expression.

To examine the functional role of circDUSP1 in TNBC cells, rescue assays were conducted by co-transfecting miR-429 mimics or inhibitors alongside circDUSP1 overexpression or knockdown vectors into MDA-MB-231 and MDA-MB-468 cells. Expression levels of circDUSP1, miR-429, and DLC1 mRNA were then assessed by qRT-PCR (Fig. 5D-F). The results indicated that miR-429 mimics suppressed the upregulation of DLC1 expression induced by circDUSP1 overexpression, while increasing miR-429 levels. Conversely, miR-429 inhibitors restored the expression of DLC1 following circDUSP1 knockdown, accompanied by reduced miR-429 levels. Western blot analysis confirmed that miR-429 mimics reduced DLC1 protein levels, whereas miR-429 inhibitors reversed this effect (Fig. 5G, H).

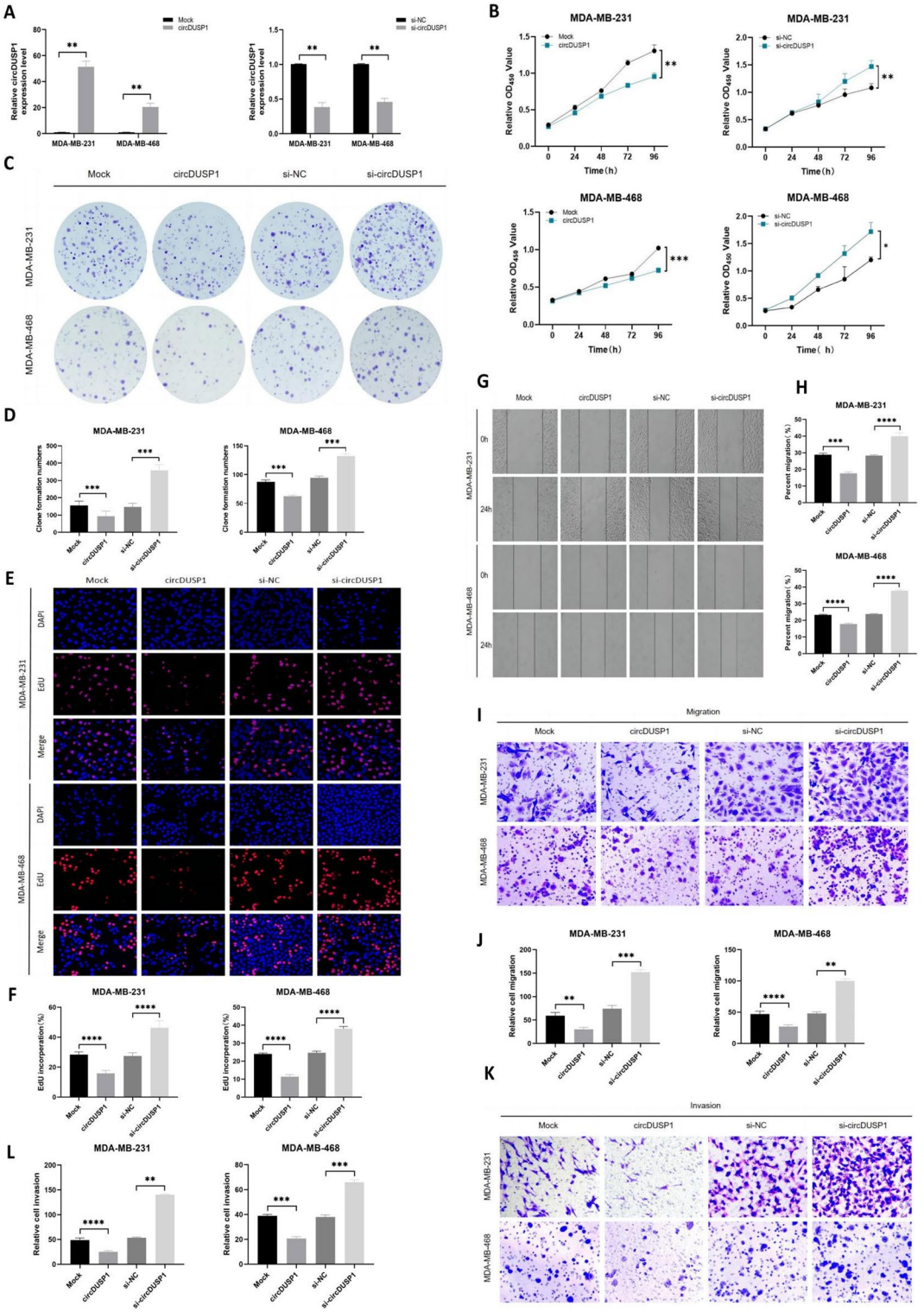

Fig. 2. circDUSP1 suppressed proliferation and metastasis of TNBC cells in vitro. (A) Two breast cancer cell lines with stable circDUSP1 overexpression and knockdown were successfully constructed, with transfection efficiency confirmed by qRT-PCR. (B) The impact of circDUSP1 on cell proliferation was assessed using the CCK-8 assay. (C-D) Colony formation assays evaluated circDUSP1's influence on cell colony-forming ability, with clone numbers quantified by ImageJ. (E-F) EdU assays measured the effect of circDUSP1 on cell proliferation (scale bar: 100 μM), with proliferative cells quantified by ImageJ. (G-H) Wound healing assay assessed circDUSP1's effect on wound healing (scale bar: 100 μM), with the degree of healing quantified by ImageJ. (I-L) Transwell assays evaluated circDUSP1's impact on cell migration and invasion, with migrated and invaded cells quantified by ImageJ (scale bar: 100 μM).

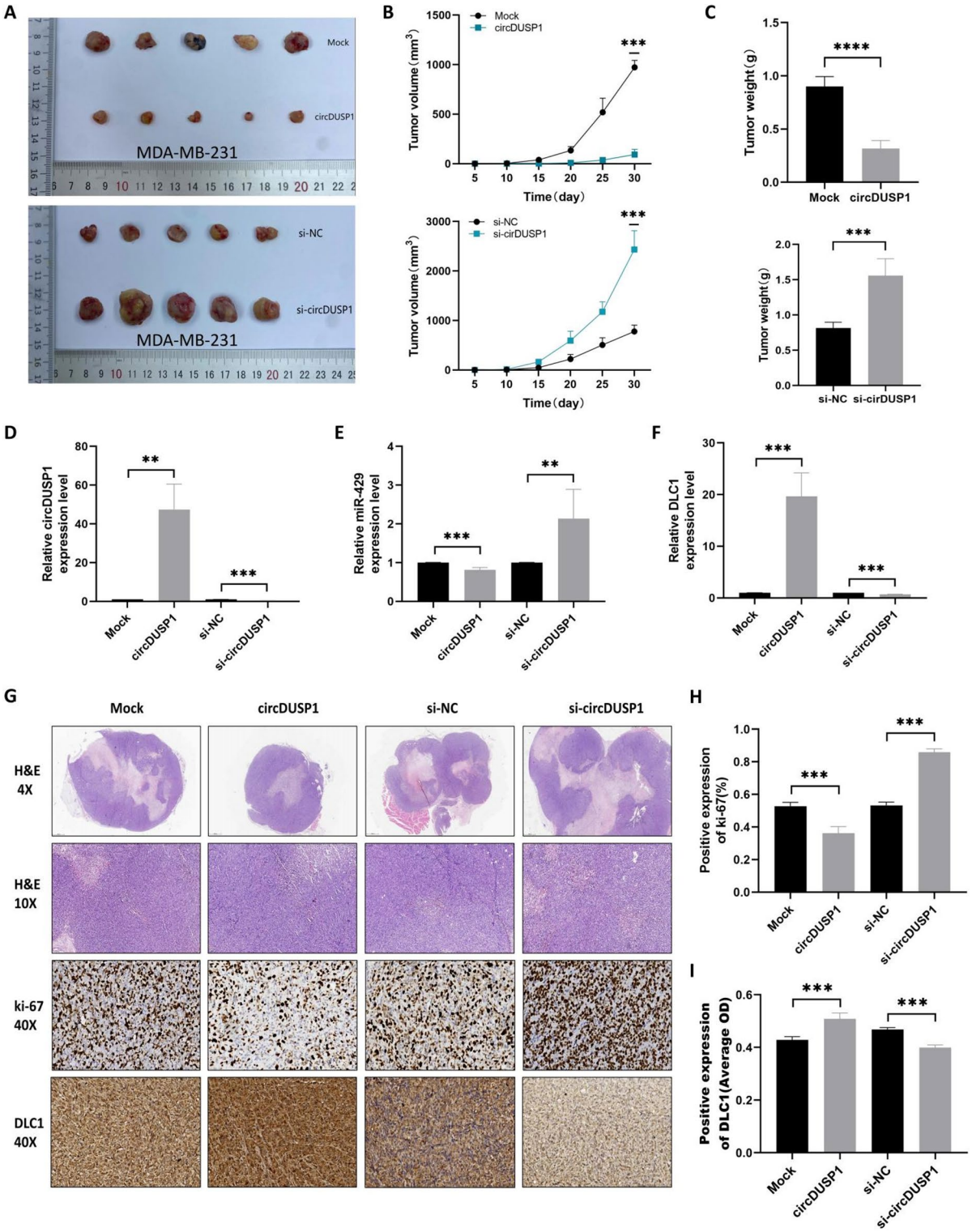

Fig. 3. circDUSP1 suppressed tumor growth in TNBC in vivo. (A) Assessment of circDUSP1's impact on tumor growth in nude mice. (B) Tumor volume changes every 5 days post-knockdown or overexpression. (C) Effects on tumor weight. (D-F) qRT-PCR analysis of circDUSP1, miR-429, and DLC1 expression levels in tumors following circDUSP1 knockdown or overexpressio. (G) Representative HE-stained tumor sections and IHC staining to assess changes in the ki-67 proliferation index and DLC1 expression. (H-I) Quantification of ki-67 positivity via ImageJ and average optical density of DLC1 IHC staining.

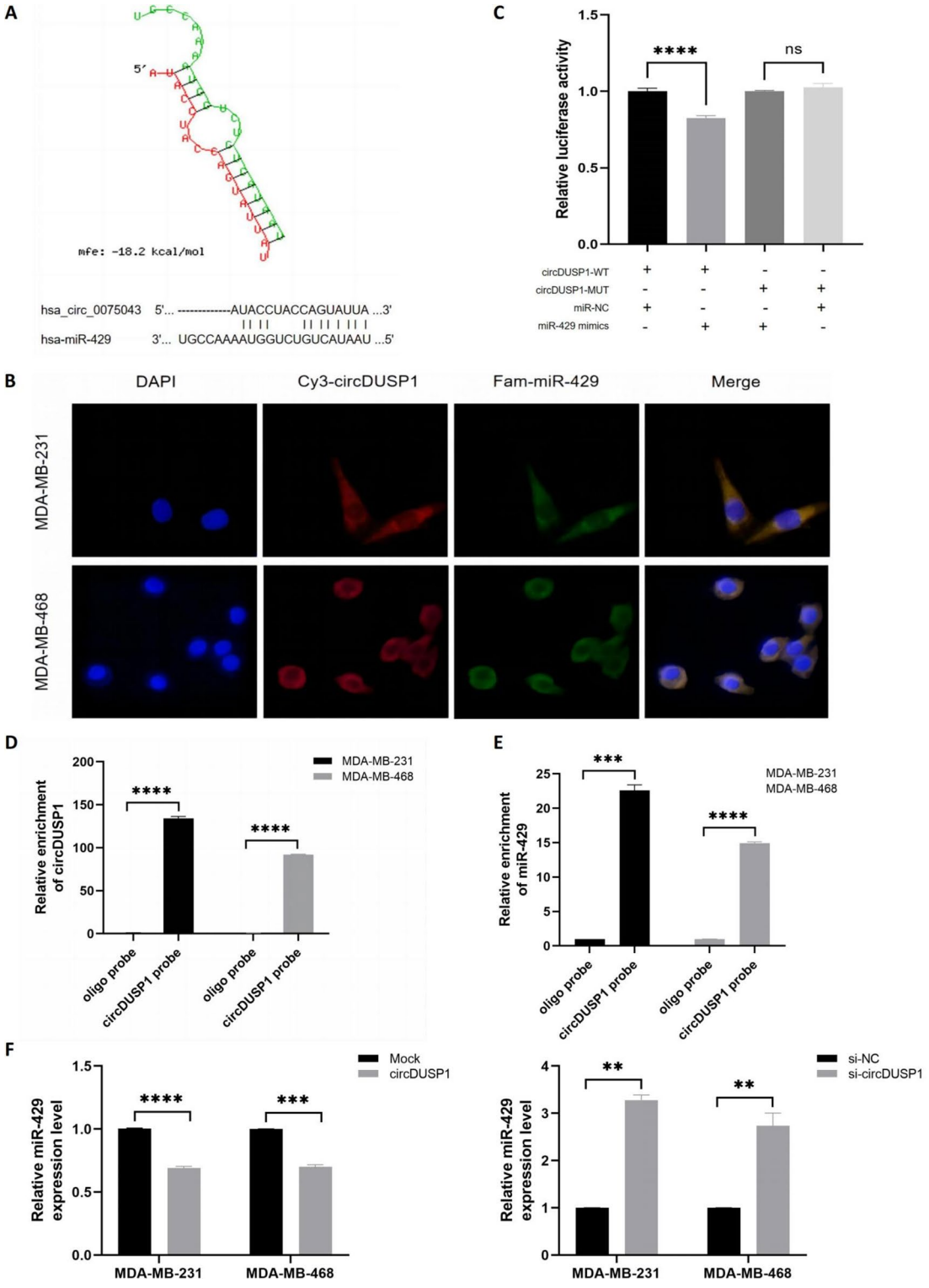

Fig. 4. In TNBC, circDUSP1 binds miR-429 and actsas a molecular sponge. (A) The *Circular RNA Interactome* database predicts circDUSP1 binding sites for miR-429. (B) FISH assay assessed the subcellular localization of circDUSP1 and miR-429 in TNBC cells (magnification: 600×; scale bar: 20 μM). (C) The interaction between circDUSP1 and miR-429 was assessed using a double luciferase reporter assay. (D-E) RNA pull-down assays demonstrate significant enrichment of circDUSP1 and miR-429 using a circDUSP1-specific probe. (F) qRT-PCR was employed to measure miR-429 expression changes following circDUSP1 overexpression or knockdown.

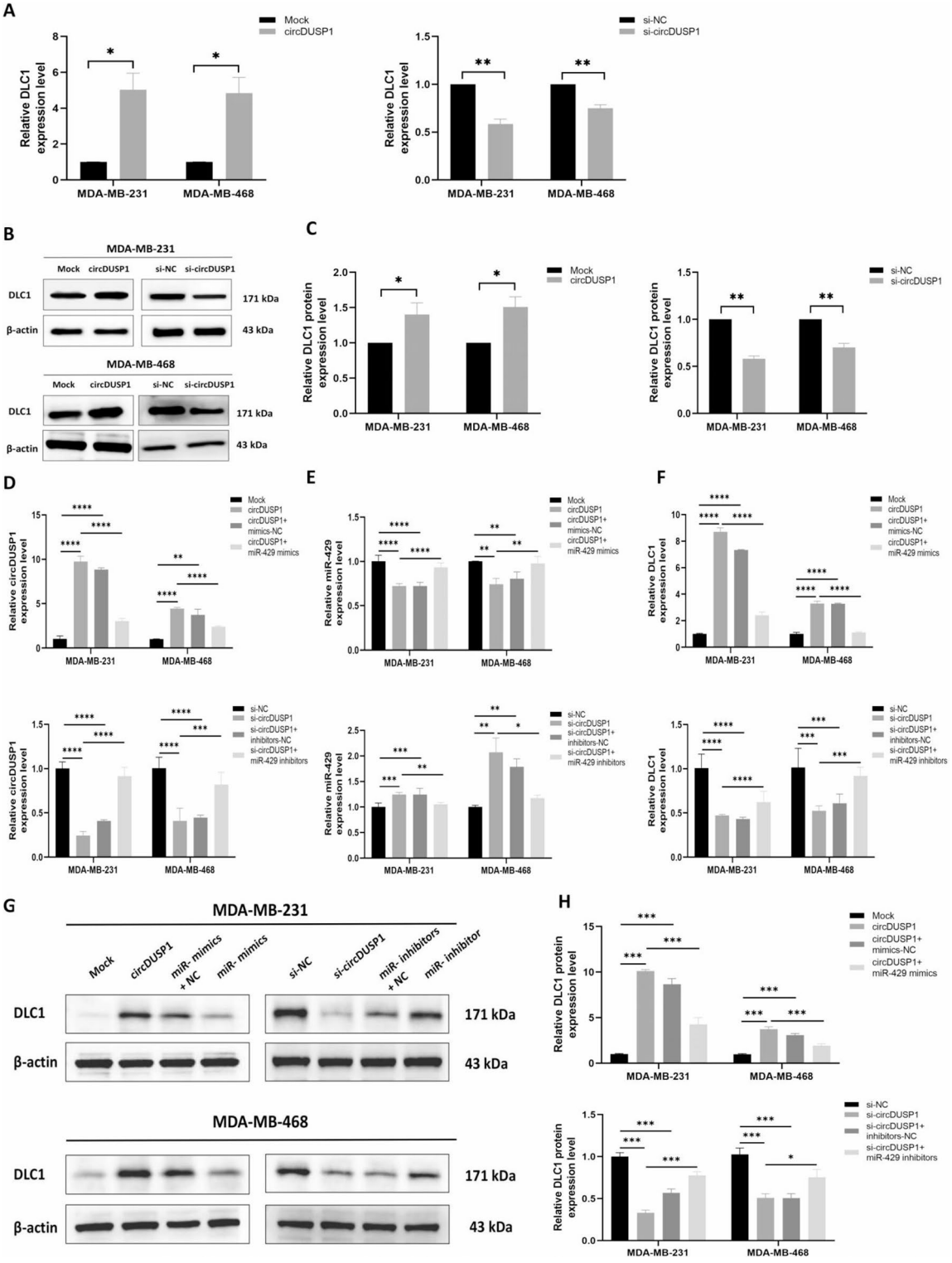

Fig. 5. circDUSP1 regulated proliferation, migration, and invasion of TNBC cells via the miR-429/DLC1 regulatory network. (A) qRT-PCR assessed DLC1 mRNA levels following circDUSP1 overexpression or knockdown. (B-C) Western blot analysis confirmed and quantified DLC1 protein expression under similar conditions. (D-F) qRT-PCR evaluated expression changes of circDUSP1, miR-429, and DLC1 in cells co-transfected with circDUSP1 overexpression or knockdown and miR-429 mimics or inhibitors. (G-H) Western blot analysis examined DLC1 protein expression in cells co-transfected with circDUSP1 and miR-429 mimics or inhibitors.

A series of rescue assays (CCK-8, colony formation, etc.) demonstrated that miR-429 mimics significantly reduced the inhibitory effects of circDUSP1 overexpression on TNBC cell proliferation, migration, and invation. Conversely, miR-429 inhibitors counteracted the promoting effects of circDUSP1 knockdown on these processes (Fig. 6A-K). These data confirm that circDUSP1 functions as a miR-429 sponge. In summary, circDUSP1 binds miR-429 via sponging, inhibiting TNBC cell processes, with miR-429 partially reversing the tumor-suppressive effects of circDUSP1.

Rescue assays demonstrated that co-transfection of circDUSP1 and miR-429 counteracted the inhibitory effects of circDUSP1 overexpression on TNBC cell processes, while miR-429 inhibition reversed the promoting effect of circDUSP1 knockdown on TNBC cell growth, migration, and invasion.

Discussion

TNBC is a highly aggressive and recurrent subtype of breast cancer[15], characterized by its poor prognosis and limited treatment options. Current therapeutic strategies primarily rely on a combination of chemotherapy, surgery, and radiotherapy[16]. However, the high heterogeneity of TNBC and the lack of effective targeted therapies result in limited treatment efficacy and frequent drug resistance[1]. These challenges significantly complicate TNBC management and highlight the urgent need for a deeper understanding of the molecular mechanisms driving TNBC onset and progression. Identifying novel therapeutic targets and biomarkers is essential for improving treatment outcomes and prognosis. Recent studies have highlighted the significant roles of circRNA and miRNA, emerging non-coding RNAs in various cancers[17], but the specific regulatory networks involving these molecules in TNBC pathogenesis remain incompletely understood. Critically, although our prior work identified miR-429 as a promoter of TNBC cell proliferation and invasion via direct targeting of the tumor suppressor DLC1[10,11], the upstream regulators controlling miR-429 activity within this oncogenic pathway were unknown. This gap in understanding the molecular hierarchy regulating the miR-429/DLC1 axis represents a key obstacle in developing targeted interventions. Therefore, based on the ceRNA hypothesis, this study examined the upstream regulatory mechanisms of miR-429 in modulating DLC1 in TNBC. Identifying circDUSP1 as a critical upstream regulator of miR-429 in TNBC. Demonstrating that circDUSP1 promotes TNBC cell proliferation, migration, and invasion by acting as a molecular sponge for miR-429, thereby de-repressing DLC1 expression. Establishing the circDUSP1/miR-429/DLC1 regulatory network as a potential therapeutic target.

Our study demonstrates that circDUSP1 acts as a tumor suppressor in TNBC. Functional assays revealed that circDUSP1 overexpression significantly inhibited TNBC cell (MDA-MB-231, MDA-MB-468) proliferation, migration, and invasion in vitro and in vivo, while its knockdown promoted these malignant phenotypes, underscoring its critical role in TNBC progression. Mechanistically, circDUSP1 directly sponges miR-429 to suppress its activity, thereby upregulating the miR-429 target gene DLC1. Rescue experiments confirmed that miR-429 overexpression partially reversed circDUSP1's tumor-suppressive effects, while circDUSP1 knockdown enhanced oncogenicity via miR-429 activation. Thus, the circDUSP1/miR-429/DLC1 regulatory network is a central regulator of TNBC malignancy, where circDUSP1 constrains tumor progression by blocking miR-429–mediated DLC1 repression. Activation of this pathway plays a critical role in the proliferation, migration, and invasion of TNBC cells.

circRNAs are established regulators of cancer pathogenesis[18], with circDUSP1 recently identified as a tumor suppressor in TNBC[7]. The host gene DUSP1 is a known regulator of the MAPK pathway (modulating ERK1/2, JNK1/2, and p38) impacting proliferation and apoptosis[19], and implicated in various cancers[20]. For instance, it suppresses the progression of ESCC by inhibiting the ERK signaling pathway, while its downregulation in prostate cancer leads to MAPK pathway activation, promoting metastasis[21]. Although a functional relationship between circDUSP1 and DUSP1 exists, the specific tumor-suppressive mechanisms of its circular transcript, circDUSP1, in TNBC remained unclear. Our study directly addresses this gap, revealing a novel circDUSP1-dependent pathway distinct from canonical DUSP1/MAPK signaling.

circRNAs primarily function via miRNA interactions[22], a class of non-coding RNAs that inhibit target mRNA expression by binding to them[23]. In the context of cancer initiation and progression, miRNAs have been classified as either oncogenes or tumor suppressors and are increasingly utilized as biomarkers for cancer diagnosis and prognosis. miR-429 is critical in the pathogenesis of various cancers. It is widely involved in regulating critical processes such as cell growth, migration, invasion, and EMT[24–27]. Studies indicate that the role of miR-429 in different cancers can be either pro-oncogenic or anti-oncogenic, influenced by the tumor's genetic background and microenvironment. In TNBC, miR-429 exerts a dual function: while its downregulation enhances bone metastasis in breast cancer[28], its upregulation promotes cell proliferation, migration, and inhibits apoptosis in TNBC[29]. Our key finding elucidates a central mechanism for this duality in TNBC: circDUSP1 acts as a direct molecular sponge for miR-429. This identifies circDUSP1 as the critical regulator resolving the paradoxical role of miR-429 within TNBC primary tumor contexts.

DLC1 is a well-established tumor suppressor gene that regulates cell morphology, adhesion, and migration through modulation of small GTP-binding proteins[30]. It functions to inhibit tumor cell proliferation and migration[31], and its loss of function is strongly linked to the initiation and progression of various cancers, including liver, breast, gastric, and prostate cancers[32–35]. Gong et al.[36]. demonstrated that DLC1 suppressed prostate cancer cell proliferation via inhibition of the Rho kinase pathway. Similarly, Yang et al.[37]. showed that DLC1 overexpression significantly inhibited the proliferation of cutaneous squamous cell carcinoma. In breast cancer, Ren et al.[38]. reported a negative correlation between DLC1 expression and both osseous metastasis and poor prognosis. Crucially, we demonstrate that circDUSP1's sponging of miR-429 directly relieves the repression of DLC1 mRNA. This establishes the novel circDUSP1/miR-429/DLC1 regulatory network as the primary mechanism through which circDUSP1 exerts its tumor-suppressive effects by inhibiting proliferation, migration, and invasion in TNBC. This finding significantly extends prior knowledge of DLC1 regulation in breast cancer by identifying its upstream control via a specific circRNA-miRNA interaction.

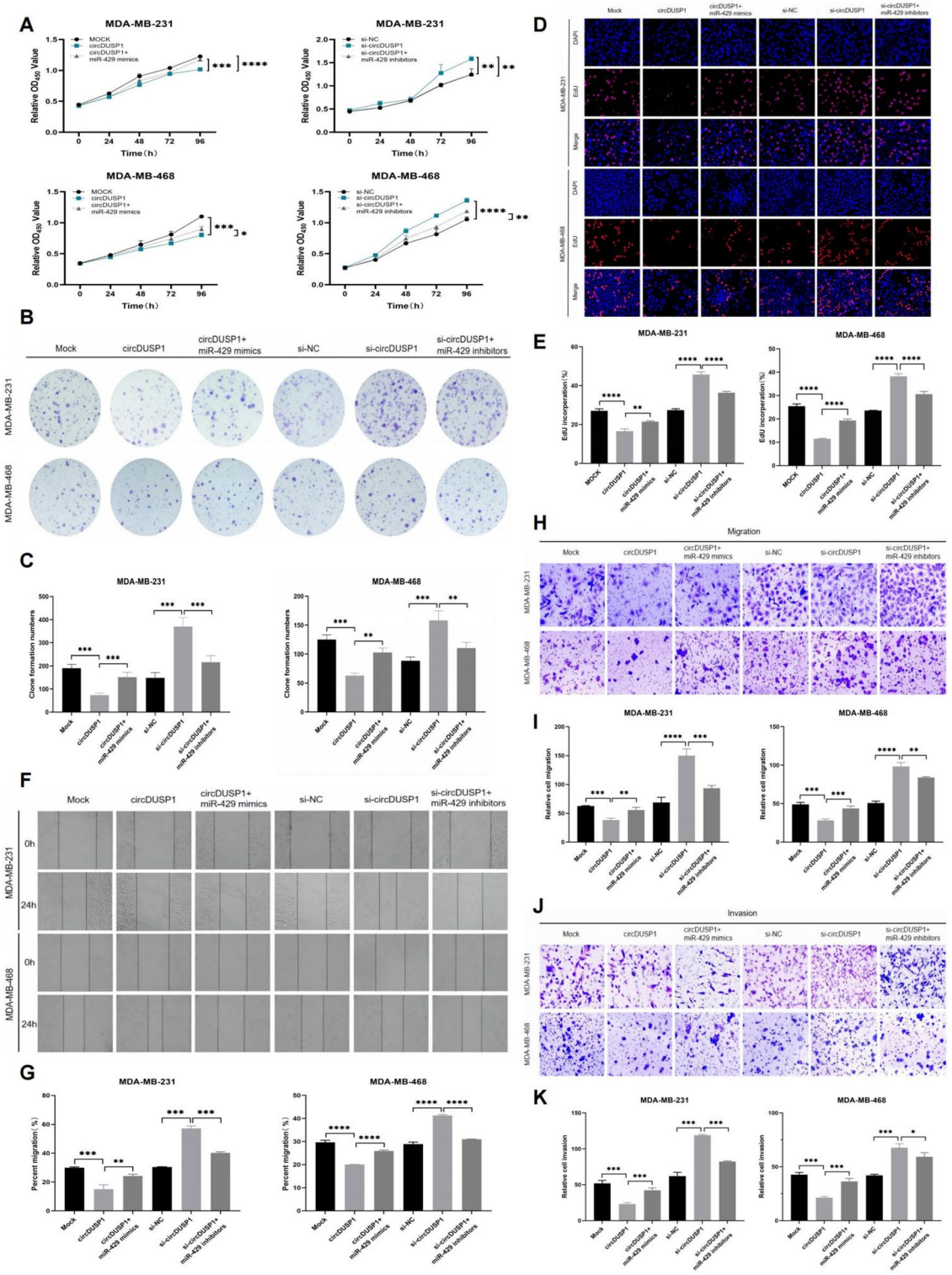

Fig. 6. circDUSP1 regulated proliferation, migration, and invasion of TNBC cells via the miR-429/DLC1 regulatory network. (A) CCK-8 assays assessed the impact of circDUSP1 and miR-429 on cell proliferation. (B-C) Colony formation assays evaluated their effects, with clone numbers quantified using ImageJ. (D-E) EdU assays measured cell proliferation, with proliferative cells quantified by ImageJ (100× magnification, scale bar: 100 μM). (F-G) Wound healing assay assessed the impact on wound healing post-co-conversion, quantified by ImageJ (100× magnification, scale bar: 100 μM). (H-K) Transwell assays evaluated cell migration and invasion following co-conversion, with migrated and invaded cells quantified using ImageJ (100× magnification, scale bar: 100 μM).

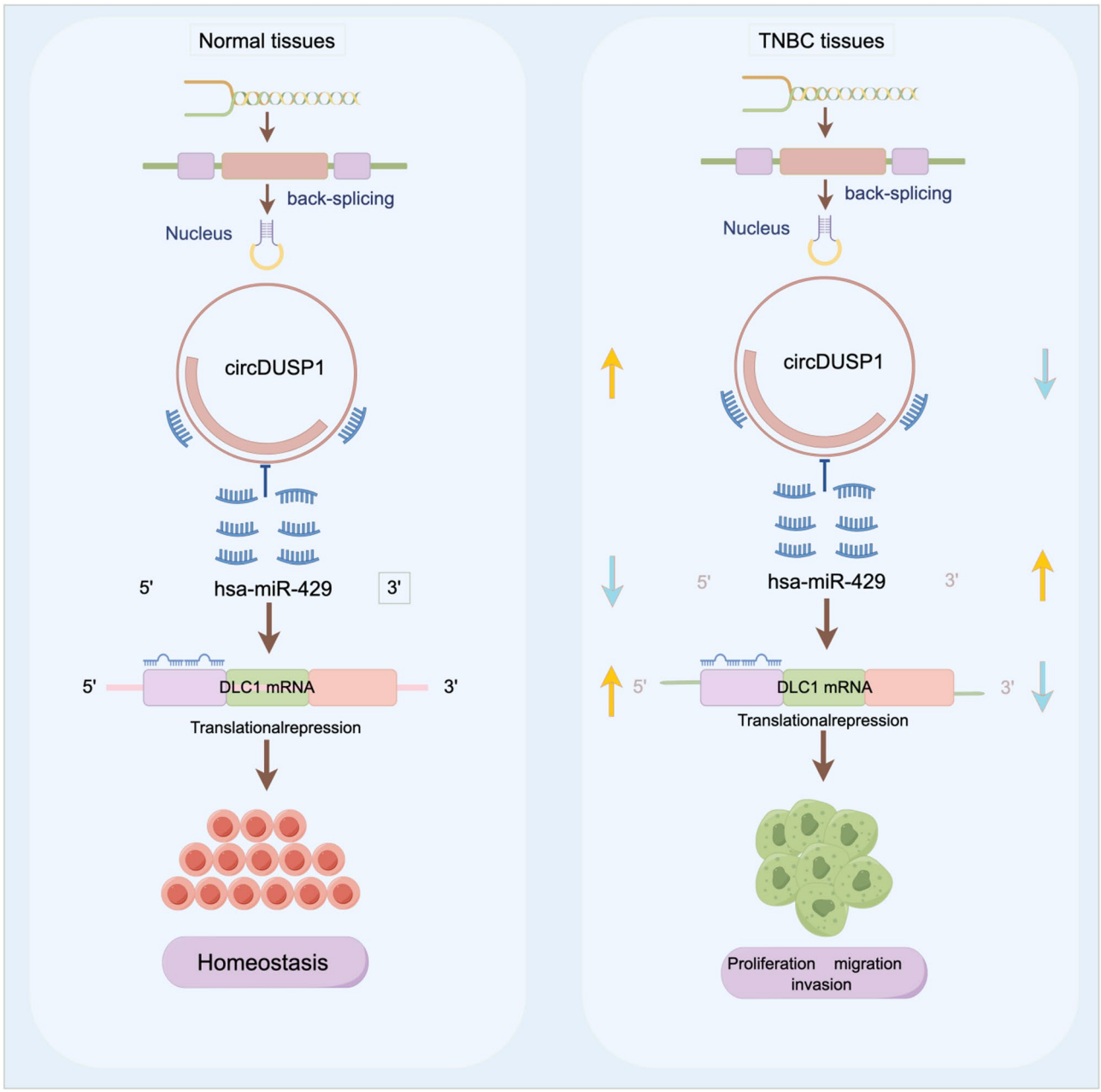

Fig. 7. circDUSP1 promotes TNBC progression by modulating miR-429/DLC1 regulatory network. As shown in the graphic model, circDUSP1 downregulated DLC1 expression by sponging miR-429, thereby promoting the proliferation, migration, and invasion in the TNBC cells.

Previous studies have shown that in TNBC, miR-429 is upregulated while DLC1 expression is downregulated, and the levels of both are associated with prognosis[10,11]. Analysis of online databases suggested that circDUSP1 may interact with multiple miR-429 binding sites, indicating its potential role as a sponge for miR-429. Based on the ceRNA hypothesis and the aforementioned finding, we proposed a functional connection between circDUSP1 and miR-429, and DLC1 in the malignant progression of TNBC. circDUSP1 has been found to be downregulated in TNBC tissues and cells, and it is negatively correlated with tumor occurrence and development[7]. To reconfirm the expression of circDUSP1 in TNBC, we detected its expression in 3 pairs of TNBC tissues (tumor vs. matched adjacent non-tumor tissues) and two cell lines (MDA-MB-231 and MDA-MB-468) using qRT-PCR. The results showed that circDUSP1 was downregulated in TNBC tissues and cells, consistent with previous reports[7]. Our study further validates the expression of circDUSP1 in TNBC; however, due to the limited number of clinical samples and cell lines tested, more TNBC samples and cell lines are needed to confirm this conclusion accurately, thereby further evaluating its clinical feasibility as a diagnostic, prognostic, and therapeutic target for TNBC.Our study has illuminated the pivotal role of the circDUSP1-miR-429-DLC1 axis in regulating TNBC cell proliferation, migration, and invasion. These findings carry significant weight in

advancing our understanding of the molecular mechanisms underpinning TNBC progression and metastasis. By elucidating the interplay between circDUSP1, miR-429, and DLC1, we have unearthed a novel signaling pathway that could be harnessed for therapeutic intervention. The clinical potential of targeting this axis—such as by inhibiting miR-429 expression or restoring the function of circDUSP1 and DLC1—could effectively suppress TNBC cell proliferation, migration, and invasion. Furthermore, circDUSP1 shows promise as a diagnostic biomarker and for monitoring treatment efficacy in TNBC, underscoring its significant clinical potential.

Although this study revealed the potential mechanism by which circDUSP1 affects TNBC cell proliferation, migration, and invasion through the miR-429/DLC1 regulatory network, there are still several limitations. First, we validated the role of the circDUSP1/miR-429/DLC1 regulatory network in TNBC proliferation using cell and animal models, but further studies are needed to investigate its impact on TNBC metastasis in vivo. Additionally, the clinical sample size for TNBC was small, which may affect the conclusions. Expanding the clinical cohort size is necessary to evaluate the clinical feasibility of these molecules as therapeutic targets and to validate the prognostic value of circDUSP1 using patient survival data. Second, this study initially uncovered the inter-regulatory relationship between circDUSP1, miR-429, and DLC1, focusing on the ceRNA mechanism, but did not investigate the downstream signaling pathways modulated by DLC1 as a consequence of this axis. Supplementing with activity detection of related pathway proteins would help to better understand its functions and complete the mechanistic explanation. Finally, previous reports indicate that the DLC1 domain can inactivate small GTP proteins, thereby maintaining normal cellular function. Therefore, we can further verify whether the activation status/activity of small GTPase proteins mediates the effects of the circDUSP1/miR-429/DLC1 regulatory network on cell proliferation, migration, and invasion, and whether it participates in the regulation of the circRNA-miRNA-mRNA network.

Future research should focus on further exploring the potential of the circDUSP1-miR-429-DLC1 regulatory network in TNBC therapy and diagnosis. For example, we can conduct in-depth studies on the stability and expression regulation of circDUSP1 in TNBC cells to clarify its mechanism of action as a ceRNA. We can also conduct preclinical experiments to evaluate the safety and efficacy of miR-429 inhibitors or circDUSP1/DLC1 expression vectors as potential therapeutic agents. At the same time, we can explore the potential of using the circDUSP1-miR-429-DLC1 regulatory network as a biomarker for early diagnosis and prognosis prediction of TNBC. This can be achieved by detecting the expression levels of these molecules in clinical samples and analyzing their correlation with TNBC progression and patient clinical outcomes. In the long term, we can conduct clinical trials to verify the therapeutic efficacy of targeting the circDUSP1-miR-429-DLC1 regulatory network in TNBC patients. This will provide a more accurate assessment of its clinical application value and help develop more effective therapeutic strategies for TNBC.

In summary, our study is the first to reveal the crucial role of the circDUSP1-miR-429-DLC1 regulatory network in the proliferation, migration, and invasion of TNBC cells. Prior research has not examined this specific network's function in TNBC. By demonstrating that circDUSP1 acts as a ceRNA to regulate miR-429, which subsequently affects DLC1, we have identified an unknown molecular mechanism that drives TNBC development. This new insight not only enriches our understanding of the complex regulatory networks in TNBC, but also offers a new perspective for developing targeted therapies. Future research will focus on identifying other downstream targets of miR-429 and exploring the upstream mechanisms leading to circDUSP1 downregulation. This will help us better understand the full scope of these regulatory networks and identify additional therapeutic targets.

Data availability

The original contributions presented in the study are included in the article/ Supplementary Material . Further inquiries can be directed to the corresponding author. Figures 1E and 7 are drawn and exported through the online website (FIG Graw2.0,https://www.figdraw.com/〉,and the export copyright ID is TOWUWb7932, SPO YO79c06. The datasets generated and / or analyzed during the current study are available at the GenBank, the GenBank accession numbers: BankIt2929803 1HSA PV176472、BankIt2929803 3HSA PV176473.

Received: 3 March 2025; Accepted: 11 July 2025
Published online: 20 July 2025

References

1. Wahba, H. A. & El-Hadaad, H. A. Current approaches in treatment of triple-negative breast cancer. *Cancer Biol. Med.* **12** (2), 106–116 (2015).
2. Bianchini, G. et al. Treatment landscape of triple-negative breast cancer - expanded options, evolving needs. *Nat. Rev. Clin. Oncol.* **19** (2), 91–113 (2022).
3. Pluta, R. & Espinosa, M. Antisense and yet sensitive: copy number control of rolling circle-replicating plasmids by small RNAs. *Wiley Interdiscip Rev. RNA*. **9** (6), e1500 (2018).
4. Salmena, L. et al. A CeRNA hypothesis: the Rosetta stone of a hidden RNA. *language? Cell.* **146** (3), 353–358 (2011).
5. Vo, J. N. et al. The landscape of circular RNA in Cancer. *Cell* **176** (4), 869–881e13 (2019).
6. Salzman, J. et al. Circular RNAs are the predominant transcript isoform from hundreds of human genes in diverse cell types. *PLoS One*. **7** (2), e30733 (2012).
7. Huang, S. et al. CircDUSP1 regulates tumor growth, metastasis, and Paclitaxel sensitivity in triple-negative breast cancer by targeting miR-761/DACT2 signaling axis. *Mol. Carcinog.* **62** (4), 450–463 (2023).
8. Ying, S. Y., Chang, D. C. & Lin, S. L. The MicroRNA (miRNA): overview of the RNA genes that modulate gene function. *Mol. Biotechnol.* **38** (3), 257–268 (2008).
9. Ambros, V. The functions of animal MicroRNAs. *Nature* **431** (7006), 350–355 (2004).
10. Li, Y. et al. The oncogenic miR-429 promotes triple-negative breast cancer progression by degrading DLC1. *Aging (Albany NY)*. **15** (18), 9809–9821 (2023).

11. Li, Y. *Effects of miR-429 Targeting DLC1 on the Proliferation,migration and Invasion of Triple Negative breast[D]* (Zunyi Medical University, 2023).
12. Zhang, Y. & Li, G. A tumor suppressor DLC1: the functions and signal pathways. *J. Cell. Physiol.* **235** (6), 4999–5007 (2020).
13. Yuan, B. Z. et al. Cloning, characterization, and chromosomal localization of a gene frequently deleted in human liver cancer (DLC-1) homologous to rat RhoGAP. *Cancer Res.* **58** (10), 2196–2199 (1998).
14. Tripathi, B. K. et al. Receptor tyrosine kinase activation of RhoA is mediated by AKT phosphorylation of DLC1. *J. Cell. Biol.* **216** (12), 4255–4270 (2017).
15. Harbeck, N. & Gnant, M. Breast cancer. *Lancet* **389** (10074), 1134–1150 (2017).
16. Guadagni, A. et al. Tackling triple negative breast cancer with HDAC inhibitors: 6 is the isoform! *Eur. J. Med. Chem.* **279**, 116884 (2024).
17. Hashemi, M. et al. Emerging roles of CircRNA-miRNA networks in cancer development and therapeutic response. *Noncoding RNA Res.* **10**, 98–115 (2024).
18. Zhou, R. et al. Circular RNAs (circRNAs) in cancer. *Cancer Lett.* **425**, 134–142 (2018).
19. Shen, J. et al. Role of DUSP1/MKP1 in tumorigenesis, tumor progression and therapy. *Cancer Med.* **5** (8), 2061–2068 (2016).
20. Bermudez, O., Pagès, G. & Gimond, C. The dual-specificity MAP kinase phosphatases: critical roles in development and cancer. *Am. J. Physiol. Cell. Physiol.* **299** (2), C189–202 (2010).
21. Wang, J. et al. Arntl-induced upregulation of DUSP1 inhibits tumor progression in esophageal squamous cell carcinoma by inactivating ERK signaling. *Cancer Biol. Ther.* **25** (1), 2408042 (2024).
22. Ben, S. et al. PiRNA PROPER suppresses DUSP1 translation by targeting N6-Methyladenosine-Mediated RNA circularization to promote oncogenesis of prostate Cancer. *Adv. Sci. (Weinh).* **11** (33), e2402954 (2024).
23. Tay, Y., Rinn, J. & Pandolfi, P. P. The multilayered complexity of CeRNA crosstalk and competition. *Nature* **505** (7483), 344–352 (2014).
24. Bilski, M. et al. miR-200 family as new potential prognostic factor of overall survival of patients with WHO G2 and WHO G3 brain gliomas. *Sci. Rep.* **14** (1), 29345 (2024).
25. Kong, X. et al. 53BP1 suppresses epithelial-mesenchymal transition by downregulating ZEB1 through microRNA-200b/429 in breast cancer. *Cancer Sci.* **106** (8), 982–989 (2015).
26. Wu, G. et al. miR-429 suppresses cell growth and induces apoptosis of human thyroid cancer cell by targeting ZEB1. *Artif. Cells Nanomed. Biotechnol.* **47** (1), 548–554 (2019).
27. Fan, J. Y. et al. miR-429 is involved in regulation of NF-κBactivity by targeting IKKβ and suppresses oncogenic activity in cervical cancer cells. *FEBS Lett.* **591** (1), 118–128 (2017).
28. Ye, Z. B. et al. miR-429 inhibits migration and invasion of breast cancer cells in vitro. *Int. J. Oncol.* **46** (2), 531–538 (2015).
29. Bi, M. et al. Ln RNA LINC01234 promotes triple-negative breast cancer progression through regulating the miR-429/SYNJ1 axis. *Am. J. Transl Res.* **13** (10), 11399–11412 (2021).
30. Kim, T. Y. et al. Effects of structure of Rho GTPase-activating protein DLC-1 on cell morphology and migration. *J. Biol. Chem.* **283** (47), 32762–32770 (2008).
31. Joshi, R. et al. DLC1 SAM domain-binding peptides inhibit cancer cell growth and migration by inactivating RhoA. *J. Biol. Chem.* **295** (2), 645–656 (2020).
32. Wong, C. M. et al. Rho GTPase-activating protein deleted in liver cancer suppresses cell proliferation and invasion in hepatocellular carcinoma. *Cancer Res.* **65** (19), 8861–8868 (2005).
33. Ullmannova, V. & Popescu, N. C. Expression profile of the tumor suppressor genes DLC-1 and DLC-2 in solid tumors. *Int. J. Oncol.* **29** (5), 1127–1132 (2006).
34. Kim, T. Y. et al. Transcriptional Silencing of the DLC-1 tumor suppressor gene by epigenetic mechanism in gastric cancer cells. *Oncogene* **22** (25), 3943–3951 (2003).
35. Zhou, X., Yang, X. Y. & Popescu, N. C. Synergistic antineoplastic effect of DLC1 tumor suppressor protein and histone deacetylase inhibitor, suberoylanilide hydroxamic acid (SAHA), on prostate and liver cancer cells: perspectives for therapeutics. *Int. J. Oncol.* **36** (4), 999–1005 (2010).
36. Gong, H. et al. Deleted in liver cancer 1 suppresses the growth of prostate cancer cells through inhibiting Rho-associated protein kinase pathway. *Asian J. Urol.* **10** (1), 50–57 (2023). Epub 2022 Jan 12.
37. Yang, C. et al. DLC1 as a regulator of proliferation, invasion, cell cycle, and apoptosis in cutaneous squamous cell carcinoma. *Tumour Biol.* **34** (5), 2633–2643 (2013).
38. Ren, G. & Li, G. Tumor suppressor gene DLC1: its modifications, interactive molecules, and potential prospects for clinical cancer application. *Int. J. Biol. Macromol.* **182**, 264–275 (2021).

Acknowledgements

We sincerely thanks to all the participants in this study. We thank the Affiliated Hospital of Zunyi Medical University for providing samples of breast tissue. Thanks to FIG Graw2.0 for providing us with the mapping website.

Author contributions

C.J., X.T., and S.L. performed cell proliferation, migration, and invasion assays; J.Z. conducted bioinformatics analysis of circRNA-miRNA networks; J.L. and T.X. established the xenograft mouse models and performed histological evaluations; C.J. and X.T. prepared figures and tables; J.W. secured funding and supervised the project; C.J. and J.W. wrote the original draft; All authors (C.J., X.T., S.L., J.Z., J.L., T.X., J.W.) reviewed and edited the manuscript.

Funding

.This study was supported by Medical Research Union Found for High-quality health development of Guizhou Province(grant No.2024GZYXKYJJXM0029), Health Commission of Guizhou Province(grant No.gzwjkj2020-1-175), Hospital fund of Affiliated Hospital of Zunyi Medical University [grant No.Yuan Zi(2017)14 Hao], Zunyi Science and Technology Program [grant No. ZunShiKeHe HZ Zi(2024)194 Hao].

Declarations

Ethics approval and consent to participate

Confirm that informed consent was obtained from the patients for the collection of all samples, and the review approval was obtained from the Ethics committee of Zunyi Medical University (Approval #KLLY-2021-028) and strictly complied with the ethical requirements of the Declaration of Helsinki. We performed the animal

studies following the ARRIVE guidelines. All the animal studies were performed following the Guidelines for the Care and Use of Laboratory Animals and were approved by the Ethics Committee of the Affiliated Hospital of Zunyi Medical University (Approval #zyfy-an-2025-0304).

Competing interests

The authors declare no competing interests.

Additional information

Supplementary Information The online version contains supplementary material available at https://doi.org/10.1038/s41598-025-11621-7.

Correspondence and requests for materials should be addressed to J.W.

Reprints and permissions information is available at www.nature.com/reprints.

Publisher's note Springer Nature remains neutral with regard to jurisdictional claims in published maps and institutional affiliations.